International Journal of Mass Spectrometry 299 (2011) 64–70

Contents lists available at ScienceDirect

International Journal of Mass Spectrometry

journal homepage: www.elsevier.com/locate/ijms

Fast side-chain losses in keV ion-induced dissociation of protonated peptides

Sadia Bari, Ronnie Hoekstra, Thomas Schlathölter*

KVI Atomic and Molecular Physics, University of Groningen, Zernikelaan 25, 9747AA Groningen, The Netherlands

ARTICLE INFO

Article history:
Received 21 June 2010
Received in revised form
20 September 2010
Accepted 21 September 2010
Available online 29 September 2010

Keywords:
Peptide
Peptide fragmentation
Ion collision
RF trap
Electrospray ionization
Resonant electron capture

ABSTRACT

In this paper, we compare ionization and dissociation of a series of singly and doubly protonated peptides, namely leucine enkephalin, bradykinin, LHRH and substance P as induced by collisions with keV H^+, He^+ and He^{2+}. For all peptides under study, the fragmentation pattern depends strongly on the electronic structure of the projectile ions. Immonium ions, side-chains and their fragments dominate the spectrum whereas fragments due to peptide backbone cleavage are weak or even almost absent for He^+. Here, resonant electron capture from the peptide is ruled out and only interaction channels accompanied by much higher excitation contribute. Cleavage of the side-chain linkage appears to be a process alternative to backbone fragmentation occurring after internal vibrational redistribution of excitation energy. Depending on the peptide, this process can lead to the loss of a side-chain cation (leucine enkephalin, LHRH) or a neutral side-chain (substance P).

1. Introduction

In a recent article, we have introduced the technique of keV ion-induced dissociation (KID) for mass spectrometric peptide analysis [1]. Sequencing and protein identification by means of mass spectrometric techniques is a powerful tool. Usually the analysis is based on excitation by multiple collisions with inert gas atoms (collision-induced dissociation, CID [2–4]) or surfaces (surface induced dissociation, SID [5,6]), on electron capture (electron capture dissociation, ECD [7–9]), on blackbody infrared radiation [10,11] and on laser light [12,13]. In KID, interactions of keV ions with biomolecules can lead to particularly high excitation energies, since collisions are governed by (multiple) electron capture (i.e., gentle electron transfer from the molecule to the ion) and electronic stopping (i.e., projectile ion-induced electronic excitations of the target molecule). The initial excitation is always occuring on a few fs-timescale.

Until recently, such keV ion collision studies were limited to effusive targets of small biomolecules which are stable with respect to thermal decomposition. We have for instance studied keV ion interaction with DNA building blocks [14] and amino acids [15]. More complex neutral systems have until now only been accesible by investigation of keV ion collisions with biomolecular clusters [16]. An opportunity to study collisions with more complex biomolecules is the use of mass-selected biomolecular ions, as for instance produced by electrospray ionization [17]. Collisions of keV ionic DNA building blocks or peptides with neutral atoms have recently been studied [18–20], e.g., to investigate the influence of solvation-shells on biomolecular fragmentation. In our first KID investigation it was found that fragmentation of protonated leucine enkephalin as induced by keV ion impact leads to mass spectra dominated by immonium ions and their fragments [1]. Large fragments due to backbone scission are observed at smaller relative intensities and could be totally suppressed by using keV He^+ ions for which resonant electron capture at large distances is almost blocked.

It is the goal of this study, to show that the dominance of resonant electron capture and electronic stopping in KID of peptides is a general feature. To this end we have experimentally studied KID of three larger peptides. In the following we will present KID spectra for interactions of keV H^+, He^+ and He^{2+} ions with the peptides bradykinin (BK, Arg-Pro-Pro-Gly-Phe-Ser-Pro-Phe-Arg, $m = 1062.21$ amu), luteinizing-hormone-releasing hormone (LHRH, pGlu-His-Trp-Ser-Tyr-Gly-Leu-Arg-Pro-Gly-NH_2, $m = 1182.29$ amu), and substance P (Arg-Pro-Lys-Pro-Gln-Gln-Phe-Phe-Gly-Leu-Met-NH_2, $m = 1347.63$ amu) which will be compared to existing data on leucine enkephalin (leu-enk, amino acid sequence: Tyr-Gly-Gly-Phe-Leu, $m = 555.62$ amu). Fig. 1 displays schematic structures of the four peptides.

2. Experiment

A sketch of the setup can be found in Fig. 2. Briefly, singly and multiply protonated peptide ions were generated in the in-house

* Corresponding author. Tel.: +31 503635099; fax: +31 503634003.
E-mail address: tschlat@kvi.nl (T. Schlathölter).
URL: http://www.kvi.nl (T. Schlathölter).

1387-3806/$ – see front matter © 2010 Elsevier B.V. All rights reserved.
doi:10.1016/j.ijms.2010.09.019

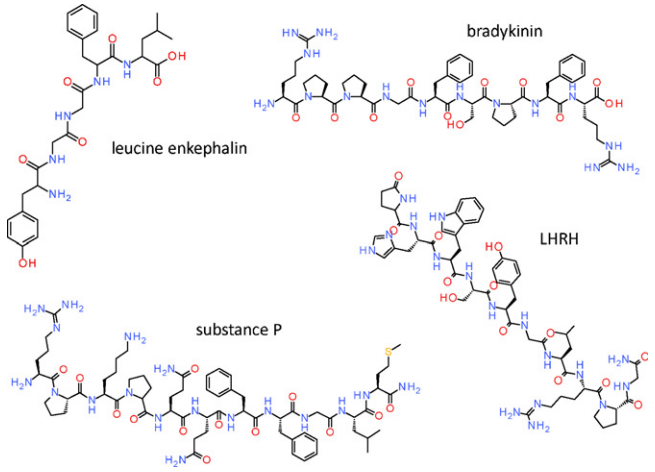

Fig. 1. Schematic structures of the four peptides under study.

built ESI source. The peptides were sprayed in methanol solutions with an addition of 1% of formic acid. Concentrations were: leu-enk: 30 μM, BK: 10 μM, LHRH: 22 μM, substance P: 15 μM. Electrosprayed ions were then guided through a collisionally focusing RF-only quadrupole followed by an RF-quadrupole mass analyzer. Eventually, the peptide ions were collected in an RF-quadrupole ion trap which they entered through an end-cap. The base pressure inside the trap chamber was 1×10^{-9} mbar. Trapping of the peptide ions requires their collisional cooling which was induced by inducing a He-buffer-gas pulse. With the buffer-gas pulse present, the estimated pressure inside the trap increased to 1×10^{-3} mbar, and the trap was typically loaded with protonated peptides over a period of a few 100 ms. When the filling cycle was completed, the ESI beam was blocked by 100 V skimmer bias and the solenoid valve, controlling the He buffer-gas flow, was closed. A delay of about 500 ms allowed the pressure in the trap to decrease to about 1×10^{-6} mbar, necessary to keep charge-changing collisions by the keV ions below 1% before reaching the trap center. A ≈100 nA beam of keV H^+, He^+ or He^{2+} projectile ions extracted from an electron cyclotron resonance ion source intersected the Paul trap through the ring electrode. Before crossing the trap region, the projectile ions were mass selected by means of a 110° dipole magnet. The protonated peptides were then exposed for about 100 ms to the ion beam. The conditions were chosen such that only about 10% of the trapped protonated peptides were dissociated by collisions with projectile ions. This ensures that only about 10% of the hit molecules are subject to two or more collisions. Note, that multiple collisions are expected to mainly produce very small fragments. Masses lower than ≈50 amu are not trapped by the trapping potential used in this study. This implies that the formation of typical small amino acid fragments such as $HCNH^+$ as e.g., observed in our earlier studies on KID of alanine, valine and glycine [21], cannot be observed in this study.

After the projectile ion pulse, a second He-buffer-gas pulse was applied to the trap, to cool energetic dissociation products. Trapped protonated peptides and their cationic dissociation products were then extracted into a linear time-of-flight (TOF) mass spectrometer ($M/\Delta M \sim 200$) by applying a bias voltage ($U_{bias} \approx 200$ V, duration: 5 μs) to the RF-trap endcaps. The ions were detected by a silhouette-type micro-channel-plate detector with the front plate biased to −5 kV and the anode kept at ground potential. The detector signal was recorded by a 1 GHz digitizer.

Despite the low background pressure and a liquid nitrogen cooled cryo-trap close to the RF-trap, contamination of the buffer-gas or neutral molecules from the ESI source may contribute to the mass spectra. To extract the mass spectrum due to peptide fragmentation only, the data acquisition was divided into successive cycles of three mass scans. In each cycle, first the TOF spectrum resulting from keV irradiation of trapped protonated peptides and neutral residual gas was recorded (inclusive scan). To obtain the net effect of keV ion irradiation upon the trapped protonated peptides, in a second scan the ECR source was switched off and a TOF spectrum of the initial trap content only was recorded. For the third scan, the ESI source was switched off and the TOF spectrum resulting from the ion-induced ionization of residual gas molecules was recorded. The latter two spectra were then subtracted from the inclusive scan. A three-scan cycle took about 3 s. To obtain the final mass spectra a series of 2000–6000 cycles was accumulated, which assures that long term fluctuations of peptide- and projectile-ion current were averaged out.

3. Results

3.1. Leucine enkephalin (leu-enk)

As already discussed in our previous publication [1], KID of leucine enkephalin leads to fragment ion distributions dominated by immonium ions and related fragments. Fig. 3 (top) displays a low-mass region of the spectrum (50–175 amu) obtained for 5 keV H^+ collisions with leucine enkephalin. Immonium ions and related ions for tyrosine (tyr, **136**, 107, 91), phenylalanine (phe, **120**, 91) and leucine (leu, **86**) dominate the spectrum. The dominance of side-chain loss is also reflected in the fact that *a*, *b*, and *c* fragments which lost the complete aromatic tyr side-chain ($m = 107$) are clearly observable (see also Fig. 3, bottom). Furthermore, intact amino acid residues for glycine (gly, marked with the one letter code G in Fig. 3) and phenylalanine (phe, marked with F) are observed.

The corresponding high m/z part of the mass spectrum for 5 keV H^+ collisions with leu-enk can be found in Fig. 3 (bottom). The peaks are generally weaker than the immonium and immonium-related ion peaks. A number of peaks due to peptide backbone scission are observed which are due to singly charged *a*, *b* and *y* fragments as well as due to an internal GF^+ fragment. Furthermore, again *a*, *b* and *c* fragments accompanied by loss of the tyr side-chain are observed. With the current mass resolution of our apparatus, we cannot resolve the b_3^+ and y_2^+ fragments which also overlap with the doubly charged singly protonated parent ion. We can thus not identify or quantify the latter. However it is likely that $(M+H)^{2+}$ is formed during KID, because of the presence of b_5^{2+} fragments.

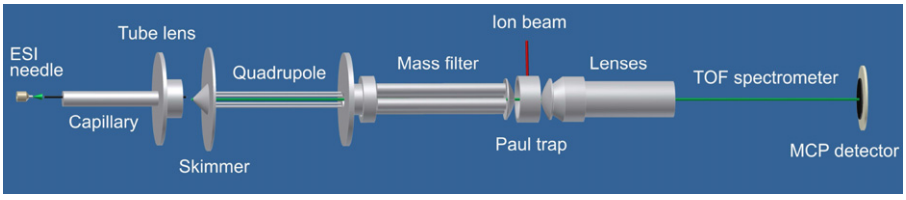

Fig. 2. Sketch of the experimental setup.

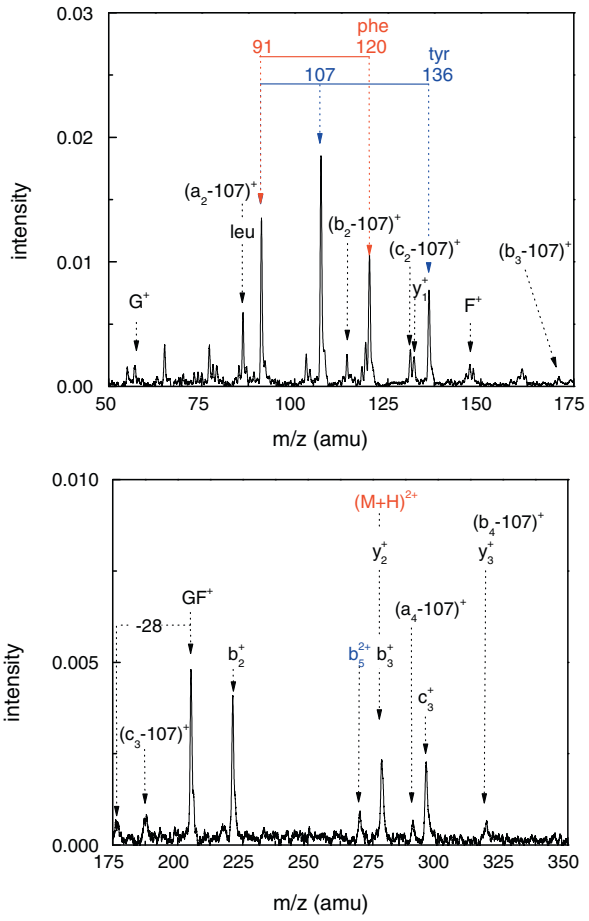

Fig. 3. KID mass spectra for 5 keV H^+ interactions with protonated leucine enkephalin. Top: Mass range of immonium and related ions up to $m/z = 175$. Immonium ions are labeled with their mass and three letter code, the respective series of related ions are grouped by lines. Amino acid residues are labeled by their one-letter code. Bottom: Larger fragments due to backbone scission. Internal fragments are labeled by the one-letter code of the respective amino acids.

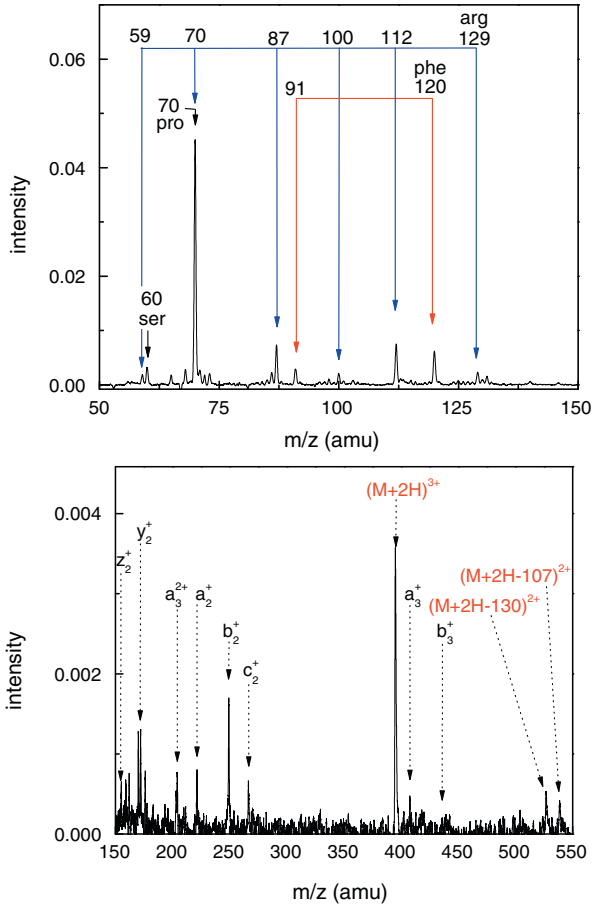

Fig. 4. KID mass spectra for 5 keV H^+ interactions with doubly protonated bradykinin. Top: Mass range of immonium and related ions up to $m/z = 150$. Bottom: Larger fragments due to backbone scission.

3.2. Bradykinin (BK)

For the larger nonapeptide bradykinin, KID of the doubly protonated species was investigated. KID spectra obtained for 5 keV H^+ impact are displayed in Fig. 4. As for leucine enkephaline, the low mass region is dominated by immonium and related ions. The arginine side-chain is prone to fragmentation at a number of bonds and some of the intermediates cyclize before subsequent loss processes. Accordingly this immonium ion is linked to a number of fragment ions (arg, **129**, 112, 100, 87, 70, 59). Phe (**120**, 91) and serine (ser, **60**) immonium ions are observed as well. The by far strongest peak is due to the proline immonium ion (pro, **70**). BK contains 3 proline residues and only two residues of phe and arg, respectively. The higher relative abundance together with the generally labile amine bond on the N-terminal side of proline residues explain the dominance of the proline immonium ion.

The dominating features in the larger mass range (Fig. 4, bottom) are the doubly protonated, triply charged BK ions, together with satellites due to loss of H_2O and CO. All types of backbone scission (*x*, *y*, *z*, *a*, *b*, *c*) are oberved with a preference for *y*, *z* and *b* fragments. Smaller fragments are observed as protonated cations, larger fragments as doubly protonated dications.

3.3. Luteinizing-hormone-releasing hormone (LHRH)

Also for LHRH, KID of the doubly protonated species was performed. Fragmentation spectra for 5 keV H^+ collisions are displayed in Fig. 5. LHRH has 8 amino acid residues with immonium ions in the mass range accesible by our trap. The low mass region of the fragmentation spectrum accordingly appears to be more complex as compared to the leu-enk and BK cases. As for BK, the peak at $m/z = 70$ which is due to the pro immonium ion and a side-chain fragment of arginine dominates the spectrum, despite the much lower relative abundance of proline in LHRH. A second peak of almost identical intensity is found at $m/z = 130$ and belongs to the tryptophan immonium series (trp, 170, **159**, 132, 130, 117, 77). $m/z = 130$ is the intact trp side-chain consisting of an indole ring with an attached methylene group. In photodissociation studies on protonated trp, Talbot et al. [22] have observed dominant production of this particularly stable fragment at high UV-photon energies (≈5.6 eV). In LHRH arg is not in a terminal position as it is for BK with the apparent consequence that no intact immonium ions are formed. However, the series of side-chain fragments shows up in the spectrum (112, 100, 87, 70, 59).

In LHRH tyr is not in an N-terminal position as in leu-enk and only leads to a weak but still visible immonium peak and associated side-chain fragments (**136**, 107, 91) with the intact side-chain $m/z = 107$ being strongest. For histidine, the immonium ion is strong and related ions are observed as well (his, 126, **110**, 82). Further immonium ions are leu (**86**), pyro-glutamic acid (pglu, **84**) and ser (60).

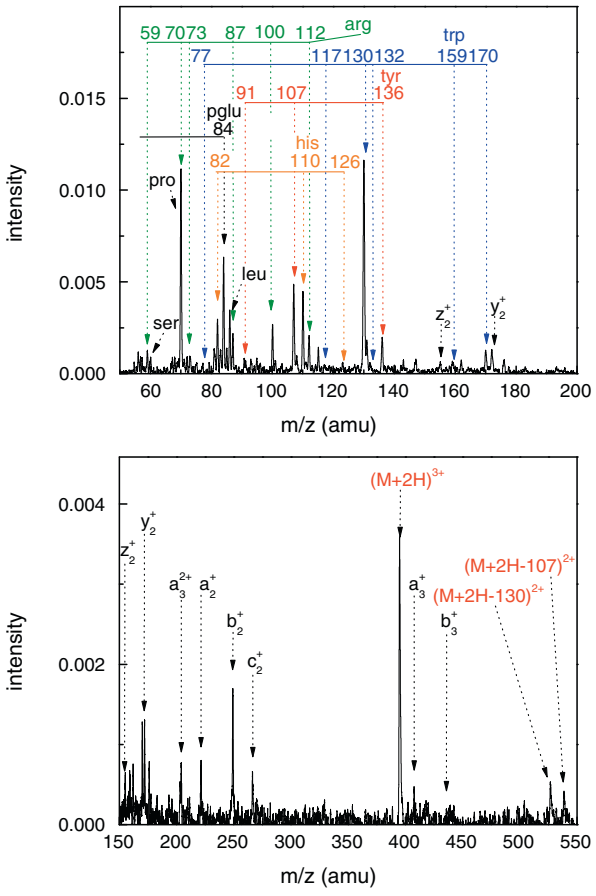

Fig. 5. KID mass spectra for 5 keV H^+ interactions with doubly protonated LHRH. Top: Mass range of immonium and related ions up to $m/z = 200$. Bottom: Larger fragments due to backbone scission.

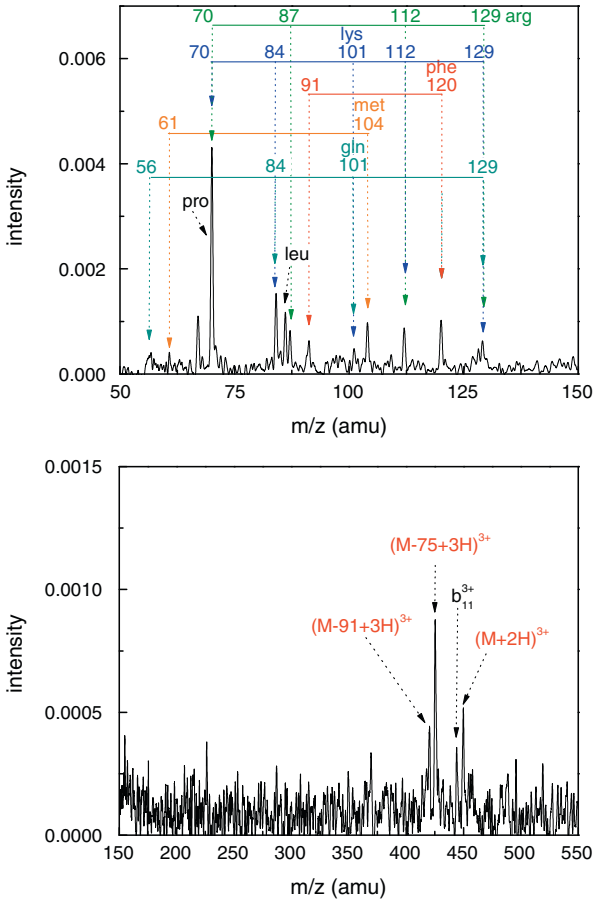

Fig. 6. KID spectra for 5 keV H^+ interactions with doubly protonated substance P. Top: Mass range of immonium and related ions up to $m/z = 150$. Bottom: Larger fragments due to backbone scission.

At larger masses, the peak due to doubly protonated triply charged LHRH dominates (Fig. 5, bottom). Two peaks due to loss of either a singly charged tyr ($m/z = 107$) or a trp ($m/z = 130$) side-chain from $(LHRH + 2H)^{2+}$ are observed as well. Furthermore, mainly singly charged peaks due to backbone scission into short fragments are observed (y, z, a, b, c).

3.4. Substance P

KID spectra for 5 keV H^+ impact on doubly protonated substance P can be found in Fig. 6. The low mass range spectrum is very rich because of the high number of different amino acid residues with immonium ions and side-chains. The spectrum is again dominated by the pro immonium ion (**70**). The peptide contains two proline residues. Furthermore, the immonium ions and related ions for arg (**129**, 112, 87,70), lysine (lys, 129, 112, **101**, 84, 70), phe ((**120**, 91), methionine (met, **104**, 61), glutamine (gln, 129, **101**, 84, 56) and leu (**86**) are observed.

The larger mass range (Fig. 6, bottom) is dominated by triply charged ions. Interestingly, the doubly protonated substance P trication which is accompanied by the b_{11}^{3+} peak is not the strongest peak. The triply protonated trication that lost the complete side-chain of the C-terminal met is the strongest peak $(M\text{-}R_M)^{3+}$. A slightly weaker peak $(M\text{-}R_F)^{3+}$ is probably due to the loss of the phe side-chain. Due to limited statistics, less intense peaks cannot be assigned unambiguously.

4. Discussion

Characteristic for keV atomic ion interations with protonated peptides are electron removal from the peptide – either by electron transfer or by direct ionzation – and high energy deposition into the peptide electronic system during fs interaction times. The two driving interaction processes are electronic stopping and electron capture from the peptide.

4.1. Electronic stopping

Electronic stopping refers to the electronic excitations of the target molecule induced by the projectile ion. The concept stems from the field of ion–solid interactions for the keV range, electronic stopping is know to be due to individual electron excitation by long range coupling to electron–hole pairs. Collective electron excitations only contribute weakly to electronic stopping and can be neglected. Numerous studies have shown that the concept of electronic stopping can also be applied to the framework of ion collisions with small molecules [23,24], polyaromatic hydrocarbons [25,26] and fullerenes [27,28]. In ion–molecule collisions, electron–hole pair production translates into exciation of valence electrons to bound excited states or to the continuum. The electronic stopping equaling the excitation energy dE deposited per trajectory interval dR can be conveniently written as a friction force [29]: $S = dE/dR = \gamma_{r_s} v$ where γ_{r_s} is the friction coefficient and v is the projectile ion velocity. If the peptide valence electrons are approximated as an electron gas, γ only depends on the

one electron radius r_s which is a function of the electron density [28].

For protonated leu-enk, we have determined the valence electron density distribution by summing up the electron densities of all valence molecular orbitals obtained by density functional theory (DFT) calculations (B3LYP, 6-31+G(d,p) basis set) for the lowest energy conformer [1]. For 5 keV H^+ impact, the maximum of the electronic stopping distribution is observed at 34 eV. This maximum is due to ion trajectories which traverse the peptide backbone or side-chains once and under steep angles. Grazing trajectories through low electron density regions lead to much lower electronic excitation. The few trajectories which traverse the peptide structure more than once or which have long pathways through high electron density regions lead to much higher electronic stopping sometimes exceeding 100 eV. Very similar electronic stopping features are expected for the other peptides. Obviously for the larger peptides the maximum deposited energy is expected to increase because of the longer trajectories through the peptide valence electron distribution. Under the experimental conditions used in this study only fragment ions with $m/z > 50$ are detected. Only grazing trajectories lead to relatively weak fragmentation into larger fragments and are thus relevant for the fragmentation patterns observed. Furthermore, this is also the class of trajectories where the ion-interaction is dominated by relatively gentle resonant electron capture from the protonated peptide.

4.2. Electron transfer

When trajectories are grazing and electronic stopping is weak, electron capture is the second major mechanism relevant in KID. In the language of atomic collisions, grazing trajectories translate to large impact parameter collisions (with a peptide constituent atom) where resonant electron capture is the dominant process. Resonant electron capture also leads to a relatively gentle ionization of a target peptide and depends strongly on the charge state and electronic structure of the projectile ion. Electron capture distances in ion-atom collisions can be estimated from the classical over-the-barrier model [30]. Within this approximation, the distance at which the keV ion captures an electron from the peptide constituent it is passing, solely depends on the target ionization energy, the charge state of the keV ion and its electronic structure.

According to the empirical formula by Budnik et al. [31] singly protonated peptides (in this case leu-enk) have an ionization energy IE of 10.9 eV, while for doubly protonated peptides IE = 12 eV is expected. For substance P, Budnik et al. measured an ionization energy as low as 11.1 eV. For IE between 10.9 eV and 12 eV

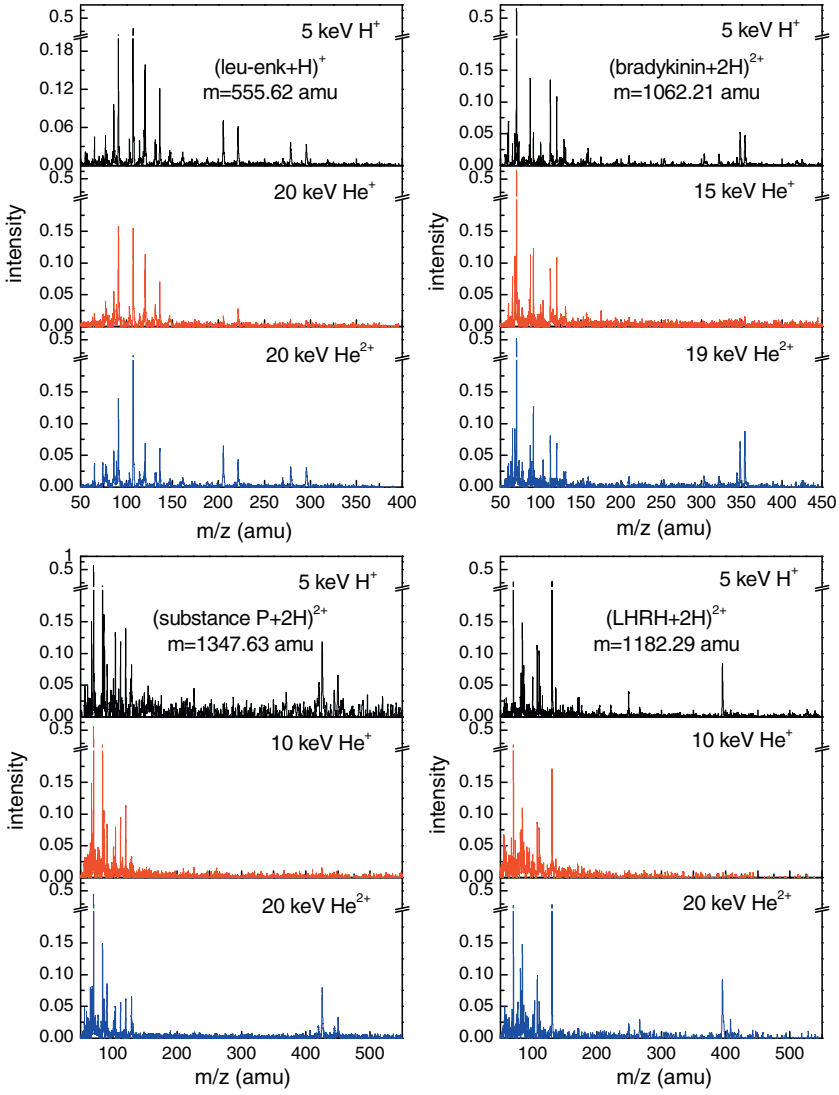

Fig. 7. KID spectra for collisions of H^+, He^+ and He^{2+} with leu-enk, BK, LHRH and substance P. The spectra are normalized to the loss of peptide ions from the trap.

the classical over-the-barrier model predicts distances between 7.5 a.u. and 6.8 a.u. for capture into a singly charged ion. For doubly charged projectile, capture distances increase to about 10 a.u. Peptide ionization can thus take place at glancing collisons.

Resonant electron capture from the peptide higher occupied molecular orbitals (HOMOs) into the projectile ion requires the availability of resonant projectile levels. For H^+ electron capture into $n = 1$ is a near resonant process allowing for relatively gentle ionization in grazing collisions. For He^+, the $n = 1$ shell at −24.6 eV is far off resonance and only becomes resonant in close collisions in which electronic stopping is high. The $n = 2$ level is far above the peptide HOMOs and thus out of reach for resonant electron capture. For He^{2+}, the third projectile ion used, electron capture from peptide HOMOs into the $n = 2$ state is a near resonant process and relatively gentle ionization in grazing collisions is again possible.

How does the presence or absence of resonant electron capture channels influence peptide dissociation? Fig. 7 displays mass spectra of the dissociation products for H^+, He^+ and He^{2+} collisions with leu-enk, BK, LHRH and substance P. The ion kinetic energies were chosen such that collision velocities are comparable. The overall trend is identical for all four peptides: for H^+ and He^{2+} besides immonium and immonium-related ions, larger fragments due to backbone scission are observed. For He^+ in which resonant capture channels are absent, larger fragments are barely present in the mass spectra. The strong influence of resonant electron capture on KID of protonated leu enk found in [1] thus seems to be a general feature. This result is also in line with our earlier studies on ion-induced dissociation of nucleobases (e.g., uracil [32]) and deoxyribose [33].

Besides the relatively strong yields of immonium ions and related fragments, KID gives rise to a number of other remarkable features in the mass spectra. For KID of protonated leu-enk, a number of N-terminal fragments are observed, which are due to backbone scission accompanied by the loss of the N-terminal tyr-side-chain ($(b_2 - 107)^+$, $(c_2 - 107)^+$, $(b_3 - 107)^+$, $(c_3 - 107)^+$, $(a_4 - 107)^+$, $(b_4 - 107)^+$). In high energy CID studies typically only side-chain loss of the amino acid at which the backbone cleavage occured is observed [3]. Moreover, even in such cases loss or fragmentation of aromatic side-chains is typically weak or even absent [3].

For a couple of tyrosine containing peptide *radical* cations on the other hand loss of $m = 106$ (probably *p*-quinomethide) has already been observed [34,35]. Nontheless, no leu-enk radicals could be produced and for the $(\text{leu-enk} + H)^+$, loss of a $m = 108$ unit was observed [34]! For the case of $(\text{RGYALG}\cdot + H)^+$ later also further collision induced dissociation into $a_5 - 106$ and $a_4 - 106$ was seen [36].

Tabarin et al. [37] have observed loss of the neutral tyr-side-chain from the protonated parent peptide after laser-induced dissociation (LID). In their study, wavelengths of 220–280 nm were chosen to induce photoabsorption by the tyr and phe side-chains. The cleavage close to the chromophore was interpreted as an indication for fast dissociation occuring before internal vibrational energy redistribution (IVR) [38]. In case of KID, electrons are resonantly captured from the HOMOs located on the tyr and phe side-chains which might induce non-ergodic fragmentation similar to LID, i.e., fast scission of the tyr C_α–C_β bond. Since in KID the electron is not excited but removed, the side-chain is positively charged and appears as the dominant feature in the mass spectrum (Fig. 3). Note, that Tabarin et al. did not observe this fragment ion. In KID resonant ionization is accompanied by excitation due to electronic stopping. After IVR this excess excitation energy apparently leads to backbone scission according to the mobile proton model [39]: Upon an increase of vibrational excitation energy, the proton attached to the remaining peptide becomes mobile and samples various protonation sites within the molecule. This way, a fragmentation pattern as expected for CID but shifted to lower masses by 107 amu occurs as part of the KID spectrum. We have recently started to investigate this process in more detail by VUV photofragmentation of leu-enk over a wide range of photon energies where the same phenomenon could be studied in more detail [40].

Table 1
Fragments due to backbone scission. Left column: KID of doubly protonated bradykinin; middle column: CID of triply charged doubly protonated bradykinin; right column: CID of triply protonated triply charged bradykinin.

$(BK+2H)^{2+}$ KID	$(BK+2H)^{3+}$ CID [41]	$(BK+3H)^{3+}$ CID [2]
		a_4^+
a_5^{2+}		a_5^+
		a_6^+
	a_7^+	
b_1^+		
b_2^+	b_2^+	b_2^+
b_4^+	b_4^+	b_4^+
b_5^{2+}	b_5^+	b_5^+
b_6^{2+}	b_6^+, b_6^{2+}	b_6^+, b_6^{2+}
		b_8^+
c_4^+	c_4^+	
c_5^{2+}		
x_1^+		
y_1^+		y_1^+
y_2^+		
y_3^+, y_3^{2+}	y_3^+	y_3^+, y_3^{2+}
y_4^{2+}		y_4^+, y_4^{2+}
		y_5^+
		y_6^+
	$(y_7 - 2)^{2+}$	y_7^+
z_1^+		
z_2^+		
z_3^{2+}		
z_4^{2+}		

KID of doubly protonated bradykinin gives rise to the richest fragmentation spectrum. Nielsen et al. [41] have collided doubly protonated 200 keV BK cations with O_2 vapor, to produce doubly protonated BK trication radicals which were subsequently subjected to CID. Since resonant electron capture from doubly protonated BK results in the same trication radical, their results are expected to be similar to our data. Tang et al. have investigated CID of triply protonated triply charged bradykinin. The fragments formed by backbone scission using the three techniques are compared in Table 1. In all cases two protons are probably located at the most basic sites, i.e., the two terminal arg residues. In all three techniques, singly and doubly charged *b*-type fragments from b_2 to b_6 with the exception of b_3 are formed. KID also leads to the additional formation of b_1^+ whereas CID of $(BK + 3H)^{3+}$ leads to additional formation of b_8^+. Complementary *y*-type ions are observed either singly or doubly charged from y_1 up to y_4 (KID) or up to y_7 (CID of $(BK + 3H)^{3+}$). CID of $(BK + 2H)^{3+}$ only leads to y_3^+ and $(y_7 - 2)^{2+}$. *b*-type and *y*-type fragments are usually assigned to charge-directed cleavage, i.e., migration of a mobile proton to the respective amide nitrogen weakening the peptide bond. The only actual pair observed in our studies is b_6^{2+}/y_3^+, formed by cleavage of the pro-6 N-terminal side.

KID and CID of $(BK + 2H)^{3+}$ both lead to the formation of a relatively strong c_4^+ fragment. Nielsen et al. [41] attribute the occurence of c_4^+ to electrostatic arguments: phe-5 is located in the middle of the peptide, with maximum distance to the two arginines that carry the charges, whereas phe-8 is close to a positive charge. The third charge is thus likely to be localized on the central phe-5 benzene side-chain leading to radical cation character of this group that weakens the phe-5 C–N bond.

Using all three approaches, one or few *a*-type ions are formed. The remarkable fact is however that KID leads to formation of small *z*-type ions which are usually observed in electron capture dissociation (ECD, [7]), i.e., electron capture by the peptide and not from the peptide, or in CID of peptide radical cations [34].

KID of doubly protonated LHRH seems to be dominated by electron capture from the tyr phenol ring or from the trp indol group: Both intact groups form strong peaks in the spectrum (107, 130) and are also observed as loss peaks from the intact doubly protonated LHRH dication. As for leu-enk, electron removal from one of the rings followed by prompt loss of the charged group seems to be an important channel. *a*, *b* and *c* N-terminal fragments are observed, all of which are due to backbone scission on the N and C side of trp. As C-terminal fragments, only y_2^+ and z_2^+ are strong, implying fragmentation on the N-terminal side of the pro residue.

For substance P, side-chains again seem to play an important role. Here, KID leads to loss of the phe side-chain (91) containing a benzene ring as well as the met side-chain (75) containing a S atom. We observe trications that lost the respective groups, i.e., bond scission does not involve a charge separation as it did for leu-enk and LHRH. Consequently, in the fragmentation pattern the respective side-chain peaks are either absent (75) or weak (91).

5. Conclusion

We have studied keV ion-induced dissociation (KID) of 4 selected protonated peptides leucine enkephalin, bradykinin, LHRH and substance P, for 3 different projectile ions H^+, He^+ and He^{2+}. The interaction can be understood in terms of resonant electron capture from the peptide accompanied by electronic excitation and ultimately vibrational excitation due to electronic stopping. For He^+ projectile ions, resonant electron capture from the peptide is ruled out and accordingly only interaction channels associated with much higher peptide excitation are open, leading to more severe fragmentation. For all peptides under study, immonium ions and side-chain fragments are dominating the mass spectrum. In most cases, KID seems to induce prompt cleavage of a side-chain linkage. Ionized side-chains are either lost positively charged (leu-enk, LHRH) or in neutral form (substance P). For leu-enk, loss of the tyr side-chain is followed by "conventional" backbone fragmentation.

Acknowledgements

This experiment has been performed at the ZERNIKELEIF part of the distributed LEIF infrastructure. Support received by the European Project ITS LEIF (RII3/026015) is gratefully acknowledged.

References

[1] S. Bari, R. Hoekstra, T. Schlathölter, Peptide fragmentation by kev ion-induced dissociation, Phys. Chem. Chem. Phys. 12 (2010) 3360.
[2] X.J. Tang, P. Thibault, R.K. Boyd, Anal. Chem. 65 (1993) 2824.
[3] I.A. Papayannopoulos, The interpretation of collision-induced dissociation tandem mass spectra of peptides, Mass Spectrom. Rev. 14 (1995) 49.
[4] A.K. Shukla, J.H. Futrell, Tandem mass spectrometry: dissociation of ions by collisional activation, J. Mass Spectrom. 35 (2000) 1069.
[5] A. Mabud, M.J. Dekrey, R.G. Cooks, Surface-induced dissociation of molecular ions, Int. J. Mass Spectrom. Ion Process. 67 (1985) 285.
[6] E. Stone, K.J. Gillig, B. Ruotolo, K. Fuhrer, M. Gonin, A. Schultz, D.H. Russell, Surface-induced dissociation on a maldi-ion mobility-orthogonal time-of-flight mass spectrometer: sequencing peptides from an in-solution protein digest, Anal. Chem. 73 (2001) 2233.
[7] R.A. Zubarev, N.L. Kelleher, F.W. McLafferty, Electron capture dissociation of multiply charged protein cations. a nonergodic process, J. Am. Chem. Soc. 120 (1998) 3265.
[8] H.J. Cooper, K. Hakansson, A.G. Marshall, The role of electron capture dissociation in biomolecular analysis, Mass Spectrom. Rev. 24 (2004) 201.
[9] A. Ehlerding, C.S. Jensen, J.A. Wyer, A.I.S. Holm, P. Jorgensen, U. Kadhane, M.K. Larsen, S. Panja, J.C. Poully, E.S. Worm, H. Zettergren, P. Hvelplund, S.B. Nielsen, Influence of temperature and crown ether complex formation on the charge partitioning between z and c fragments formed after electron capture by small peptide dications, Int. J. Mass Spectrom. 282 (2009) 21.
[10] R.C. Dunbar, T. McMahon, Activation of unimolecular reactions by ambient blackbody radiation, Science 279 (1998) 194.
[11] P.D. Schnier, W.D. Price, R.A. Jockusch, E.R. Williams, Blackbody infrared radiative dissociation of bradykinin and its analogues: energetics, dynamics, and evidence for salt-bridge structures in the gas phase, J. Am. Chem. Soc. 118 (1996) 7178.
[12] M.S. Thompson, W. Cui, J.P. Reilly, Fragmentation of singly charged peptide ions by photodissociation at *l* = 157 nm, Angew. Chem. Int. Ed. 43 (2004) 4791.
[13] R. Parthasarathi, Y. He, J.P. Reilly, K. Raghavachar, New insights into the vacuum uv photodissociation of peptides, J. Am. Chem. Soc. 132 (2010) 1606.
[14] F. Alvarado, J. Bernard, B. Li, R. Bredy, L. Chen, R. Hoekstra, S. Martin, T. Schlathölter, Precise determination of 2-deoxy-d-ribose internal energies after kev proton collisions, ChemPhysChem 9 (2008) 1254–1258.
[15] S. Bari, P. Sobocinski, J. Postma, F. Alvarado, R. Hoekstra, V. Bernigaud, B. Manil, J. Rangama, B. Huber, T. Schlathölter, Fragmentation of α and β-alanine molecules by ions at bragg-peak energies, J. Chem. Phys. 128 (2008) 074306.
[16] T. Schlathölter, F. Alvarado, S. Bari, A. Lecointre, R. Hoekstra, V. Bernigaud, B. Manil, J. Rangama, B. Huber, Ion-induced biomolecular radiation damage: from isolated nucleobases to nucleobase clusters, ChemPhysChem 7 (2006) 2339.
[17] J. Fenn, Electrospray wings for molecular elephants (nobel lecture), Angew. Chem. Int. Ed. 42 (2003) 3871.
[18] B. Liu, S.B. Nielsen, P. Hvelplund, H. Zettergren, H. Cederquist, B. Manil, B.A. Huber, Collision-induced dissociation of hydrated adenosine monophosphate nucleotide ions: protection of the ion in water nanoclusters, Phys. Rev. Lett. 97 (2006) 133401.
[19] B. Liu, N. Haag, H. Johansson, H.T. Schmidt, H. Cederquist, S.B. Nielsen, H. Zettergren, P. Hvelplund, B. Manil, B.A. Huber, Electron capture induced dissociation of nucleotide anions in water nanodroplets, J. Chem. Phys. 128 (2008) 075102.
[20] H. Zettergren, L. Adoui, V. Bernigaud, H. Cederquist, N. Haag, A.I.S. Holm, B.A. Huber, P. Hvelplund, H. Johansson, U. Kadhane, M.K. Larsen, B. Liu, B. Manil, S.B. Nielsen, S. Panja, J. Rangama, P. Reinhed, H.T. Schmidt, K. Stochkel, Electron-capture-induced dissociation of microsolvated di- and tripeptide monocations: elucidation of fragmentation channels from measurements of negative ions, ChemPhysChem 10 (2009) 1619.
[21] S. Bari, F. Alvarado, J. Postma, P. Sobocinski, R. Hoekstra, T. Schlathölter, Kinetic energy releases of small amino acids upon interaction with kev ions, Eur. Phys. J. D 51 (2009) 81.
[22] F.O. Talbot, T. Tabarin, R. Antoine, M. Broyer, P. Dugourd, Photodissociation spectroscopy of trapped protonated tryptophan, J. Chem. Phys. 122 (2005) 074310.
[23] U. Werner, N.M. Kabachnik, V.N. Kondratyev, H.O. Lutz, Orientation effects in multiple ionization of molecules by fast ions, Phys. Rev. Lett. 79 (1997) 1662.
[24] N.M. Kabachnik, V.N. Kondratyev, Z. Roller-Lutz, H.O. Lutz, Multiple ionization of atoms and molecules in collisions with fast ions. II. Ion–molecule collisions, Phys. Rev. A 57 (1998) 990.
[25] E.R. Micelotta, A.P. Jones, A.G.G.M. Tielens, Polycyclic aromatic hydrocarbon processing in interstellar shocks, Astron. Astrophys. 510 (2010) a36.
[26] J. Postma, S. Bari, R. Hoekstra, A. Tielens, T. Schlathölter, Ionization and fragmentation of anthracene upon interaction with kev protons and alpha particles, Astrophys. J. 708 (2010) 435.
[27] M. Larsson, P. Hvelplund, M. Larsen, H. Shen, H. Cederquist, H.T. Schmidt, Electron capture and energy loss in ≈100 keV collisions of atomic and molecular ions on C_{60}, Int. J. Mass Spec. 177 (1998) 51.
[28] T. Schlathölter, O. Hadjar, R. Hoekstra, R. Morgenstern, Strong velocity effects in colisions of He^+ with fullerenes, Phys. Rev. Lett. 82 (1999) 73.
[29] A. Närmann, R. Monreal, P.M. Echenique, F. Flores, W. Heiland, S. Schubert, Charge exchange and energy dissipation of particles interacting with metal surfaces, Phys. Rev. Lett. 64 (1990) 1601.
[30] A. Niehaus, A classical model for multiple-electron capture in slow collisions of highly charged ions with atoms, J. Phys. B: At. Mol. Phys. 19 (1986) 2925–2937.
[31] B.A. Budnik, Y.A. Tsybin, P. Hakansson, R.A. Zubarev, J. Mass Spectrom. 37 (2002) 1141.
[32] J. de Vries, R. Hoekstra, R. Morgenstern, T. Schlathölter, C^{q+} induced ionization and fragmentation of uracil: effects of the projectile electronic structure, J. Phys. B: At. Mol. Opt. Phys. 35 (2002) 4373.
[33] F. Alvarado, S. Bari, R. Hoekstra, T. Schlathölter, Quantification of ion-induced molecular fragmentation of isolated 2-deoxy-d-ribose molecules, Phys. Chem. Chem. Phys. 8 (2006) 1922.
[34] I.K. Chu, C.F. Rodriquez, T.-C. Lau, A.C. Hopkinson, K.W.M. Siu, Molecular radical cations of oligopeptides, J. Phys. Chem. B 104 (2000) 3393.
[35] J. Laskin, Z. Yang, C. Lam, I.K. Chu, J. Laskin, Z. Yang, C. Lam, I.K. Chu, Anal. Chem. 79 (2007) 6607.
[36] Q. Sun, H. Nelson, T. Ly, B.M. Stoltz, R.R. Julian, Side chain chemistry mediates backbone fragmentation in hydrogen deficient peptide radicals, J. Proteome Res. 8 (2009) 958.
[37] T. Tabarin, R. Antoine, M. Broyer, P. Dugourd, Specific photodissociation of peptides with multi-stage mass spectrometry, Rapid Commun. Mass Spectrom. 19 (2005) 2883.
[38] Y. Hu, B. Hadas, M. Davidovitz, B. Balta, C. Lifshitz, Does IVR take place prior to peptide ion dissociation, J. Phys. Chem. A 107 (2003) 6507.
[39] B. Paizs, S. Suhai, Fragmentation pathways of protonated proteins, Mass Spectrom. Rev. 24 (2005) 508.
[40] S. Bari, O. Gonzalez-Magaña, G. Reitsma, R. Hoekstra, J. Werner, S. Schippers, T. Schlathölter, Dissociation of a free protonated peptide by VUV photons, J. Chem. Phys., submitted for publication.
[41] S.B. Nielsen, J.U. Andersen, P. Hvelplund, T.J.D. Jorgensen, M. Sorensen, S. Tomita, Int. J. Mass Spectrom. 213 (2002) 225.